Eurasian J. Sci. Eng., 2025, 11(3), 358-373
https://doi.org/10.23918/eajse.v11i3p23

Published by Tishk International University
Available at: https://eajse.tiu.edu.iq/

RESEARCH ARTICLE Open Access

Flexural Behavior of Concrete Beams Reinforced with Carbon FRP and Steel Rebars

Hamza Omar Ismael [1]*, and Omar Qarani Aziz [1]

[1] Civil Engineering Department, Salahaddin University-Erbil, Erbil, Iraq

Article History
Received: 01.07.2025
Revised: 10.02.2026
Accepted: 14.05.2026
Published: 14.05.2026
Communicated by: Asst. Prof. Dr. Thamir M. Ahmed
**Email address:*
hamzaengineer1234@gmail.com
**Corresponding Author*

Abstract: This research explores the flexural characteristics exhibited by concrete beams reinforced with either carbon fiber-reinforced polymer (CFRP) or conventional steel bars. A total of eight beams were cast, four reinforced with CFRP bars and four with steel bars, and were assessed using a four-point flexural testing method setup over an effective span of 2000 mm. Beams had a uniform height of 350 mm and a width of 150 mm to ensure a consistent reinforcement ratio. The beam designs followed the guidelines of ACI 440.1R-15 and ACI 318-19. Variables in the study were the reinforcement ratios relative to the balanced reinforcement ratio for FRP bars, and for steel, the ratio relative to the maximum allowable reinforcement. Bar type was considered a variable. Key parameters evaluated included the load at which initial cracking occurs, the maximum load the specimen can sustain, load-deflection behavior, and failure modes. Results indicated that beams reinforced with FRP bars exhibited greater deflection compared to those reinforced with steel. The ultimate load capacity was higher in steel-reinforced beams, suggesting greater stiffness of steel bars. CFRP reinforced beams (BSC) showed a greater number of cracks than the steel-reinforced beams (BSN); crack widths were wider in BSN beams than in BSC beams.

Keywords: *Reinforced Concrete Beam; Crack Pattern; Flexural Behavior; Steel Bars; FRP Bars*

1. Introduction

Concrete incorporating steel reinforcement has demonstrated enduring efficacy over the long term. However, in aggressive environments, steel reinforcements are vulnerable to corrosive deterioration, which can lead to structural deterioration, manifested as cracking, material flaking, and the detachment of steel bars from the surrounding concrete [1].

One of the primary factors affecting the service life of reinforced concrete (RC) structures is the corrosion of steel reinforcement bars, especially in structures exposed to moisture, chloride, and de-icing salt environments, such as dams, tanks, and bridges. To mitigate corrosion-related damage, steel bars are often coated or replaced with non-corrosive alternatives. Over the past four decades, fiber-reinforced polymer (FRP) bars have been increasingly used as an alternative material to steel reinforcement bars due to their corrosion resistance and high strength-to-weight ratio [2].

The utilization of composite bars has gained significant global attention and is increasing adoption within the construction sector as embedded reinforcement in concrete structures, primarily because of their ability to improve durability and extend service life. As shown in Figure 1 [3], FRP composites typically consist of high-strength fibers integrated in a lightweight polymer matrix. They are considered highly attractive for construction applications due to their corrosion resistance, low weight, high tensile strength, nonmagnetic properties, and easy installation procedure.

FRP bar reinforced concrete members generally fail in a brittle manner. Furthermore, compared to steel reinforcing bars, the modulus of elasticity of the FRP bar is significantly lower, and the bond between the FRP bar and concrete is relatively weak. Thus, larger deflections and wider crack widths are often observed in FRP bar reinforced concrete structures. Owing to the linear elastic stress-strain behavior and low modulus of elasticity of the FRP bar, the design of FRP bar reinforced concrete structures is usually controlled by the serviceability limit state requirements [4].

Previous studies by Okelo et al. [5] have shown that carbon fiber reinforced polymer (CFRP) bars can be effectively anchored in concrete using a Surface treatment with sand to facilitate enhanced mechanical engagement between materials and frictional resistance to pullout forces. Furthermore, several researchers, such as Benmokrane, B. et al. [6] and Masmoudi, A. et al. [7] have suggested that FRP bars can perform comparably to steel bars in reinforced concrete beams, although they require different design considerations. Design codes such as ACI 440.1R-15 [8] and CSA S806-12 [9] support the use of FRP stirrups as transverse reinforcement in concrete members.

Figure 1: CFRP bars [3]

2. Literature Review

FRP bars exhibit a linear-elastic tensile behavior. The material's stress–strain performance up to the limit of rupture, depicted in Figure 2 for different categories of fibers [10], is consistent with earlier observations that FRP reinforcement lacks a yielding plateau before rupture. Accordingly, FRP bars fail when exposed to tensile stresses greater than their tensile strength, with fracture often occurring as a result of fiber breakage and delamination. The tensile performance of FRP reinforcement is determined by multiple parameters, particularly the fiber volume fraction within the composite cross-section (fiber-volume fraction). Changes in this ratio can significantly influence the strength and rigidity of FRP reinforcement. Furthermore, the matrix material’s composition and the extent of manufacturing quality control notably impact the performance of FRP reinforcement. Table 1, adapted from ACI 440.1R-15, presents the typical tensile properties of FRP and steel reinforcement bars, encompassing tensile strength, elastic stiffness, and rupture strain.

Aziz, O. Q., & Taha, B. O. [11] conducted a study focusing on the flexural properties and response of high-strength concrete beams reinforced with CFRP bars. A total of 27 simply supported high-strength concrete beams reinforced with rebars underwent flexural testing under two symmetrical point loads, as illustrated in Figure 3. The key parameters evaluated in the study included the reinforcement ratio (ρ), concrete compressive strength (f'c), and the volume fraction of chopped carbon fibers (Vf). Findings demonstrated that the maximum load capacity is directly correlated with the reinforcement ratio and the concrete compressive strength. Under a service load equivalent to 30% of the ultimate load, FRC beams exhibited crack spacing about 20% narrower than that of plain concrete beams.

Rafi, M. M [12] reported the results of a mechanical performance assessment of concrete beams reinforced with CFRP tension bars and conventional steel reinforcement. The investigation emphasized the flexural performance of the beams by analyzing stress–strain relationships, deflection patterns, failure mechanisms, load resistance, and crack propagation patterns. A measurement instrument was deployed to record the beam deflections, as well as the movement and deformation

experienced by the reinforcing bars. The collapse of beams reinforced with CFRP bars was caused by the crushing of the concrete, while the steel-reinforced beams failed through concrete crushing subsequent to the yielding of tension reinforcement. Both beam categories showed approximately equal crack spacing and a similar number of cracks throughout the entire loading sequence. The bonding properties of the CFRP reinforcement were found to meet expectations. As a result of overestimating the stiffness of CFRP-reinforced beams, the ACI code equation consequently over-predicted their theoretical deflections; experimental deflections exceeded those predicted by the ACI approach.

One of the primary drawbacks inherent to all categories of FRP composites, including reinforcement bars, is their inherently brittle failure mechanism. FRP reinforcement is widely recognized for its lack of ductility and, contrary to the ductile nature of conventional steel reinforcement, does not display ductile yielding characteristics. Owing to the non-plastic nature of the material, on-site modification of FRP reinforcement is constrained by its low flexibility. The shaping process requires professional equipment operated by the manufacturer. The directional arrangement of fibers presents an additional challenge, since it has a decisive impact on the reinforcement's strength. The FRP reinforcement exhibits lower strength perpendicular to the fiber orientation than along the fibers. Also, the limited stiffness of FRP bars, indicated by their low elastic modulus, contributes to serviceability concerns, which leads to greater deflections and significant cracking within flexural components. Despite the higher upfront cost of FRP reinforcement compared to steel, the long-term cost of ownership for structures using FRP reinforcement is comparatively lower, given the notably diminished maintenance costs associated with FRP-reinforced components [13].

Hawileh, R. A., et al [14] discussed the results obtained from a laboratory-based investigation on the structural performance characteristics of carbon and basalt fiber-reinforced materials, and the hybrid composite arrangements, consisting of multiple layers, were evaluated under elevated temperature conditions. A total of 140 coupon test samples were constructed and subjected to testing as a part of the experimental program after conditioning at various temperatures between 25°C and 250°C. Results revealed a decline in the mechanical stiffness and tensile resistance of carbon and basalt laminate materials with rising temperature. Nevertheless, the carbon composite sheets exhibited a greater degree of deterioration. The experimental results further indicated that carbon laminates experienced the most significant mechanical degradation, which reached nearly 90% at 250°C. Moreover, the material rigidity and tensile load-bearing capacity measurements demonstrated that the hybrid and basalt laminates maintained superior mechanical performance under elevated temperature conditions.

FRP is described as a heterogeneous composite system and a material comprising fibers embedded in a polymeric phase substrate, as illustrated in Figure 4 [15]. The incorporation of fibers into polymer-based materials provides enhanced strength and stiffness while maintaining a lightweight structure.

Al-Shamaa [15] examined the load-bearing capacity of lightweight concrete beams reinforced with fiber-reinforced polymer (FRP) rebars under flexural stress. Eighteen rectangular beams were subjected to testing as a part of the experimental investigation with a width of 125, height of 200 mm, and length (2400 mm, 1320 mm). Out of the total number of beams, twelve comprised lightweight concrete, and six were fabricated from conventional concrete reinforced with glass fiber reinforced polymer (GFRP), basalt fiber reinforced polymer (BFRP), or steel specimens and were tested using a two-point loading configuration. The key variables considered in the experimental program were the concrete type (lightweight or normal concrete), reinforcement type (steel or FRP), FRP classification (GFRP or BFRP), and the reinforcement ratio, strength of the concrete, the ratio of shear span to effective depth (a/d), as well as the load-bearing capacity of the evaluated beams. The outcomes of the

conducted experiments demonstrated that the overall flexural behavior of the lightweight concrete beams closely mirrored that of beams made with normal concrete.

Robert, M. et al. [16] conducted an experimental investigation comparing the durability properties of BFRP rebars with those of GFRP and CFRP, focusing on their resistance to alkaline environments, durability against weather-induced degradation, and thermal resilience. Their experimental findings highlighted that CFRP possesses superior alkali resistance compared to BFRP and GFRP. The rate at which strength diminished in GFRP during natural weathering was about two times greater than that in BFRP. Results from thermal stability tests showed notable strength loss in CFRP and GFRP with increasing temperature, in contrast to BFRP, which retained around 90% of its original strength up to 600°C. Following a 2-hour exposure at 1200°C, the CFRP appeared fully molten, having entirely lost its volumetric stability, whereas the GFRP exhibited only partial loss of stability. Despite this, BFRP upheld its morphology and strength characteristics.

The evaluation of the tensile behavior of FRP reinforcement bars is significantly more complex and differs substantially from the conventional standard procedures used for steel reinforcement. Numerous factors and specific protocols must be carefully considered before conducting the testing. A primary challenge in FRP tensile testing is preventing early deterioration, leading to failure caused by points of stress amplification, which arise due to the material's low compressive strength. To mitigate localized stress intensifications near the terminations of FRP reinforcement bars, resulting from the pressure exerted by the testing apparatus, steel hollow anchors have been employed [17].

Banibayat, P.& Patnaik, A. [18] investigated the creep rupture behavior of BFRP rebars subjected to sustained loading while being exposed to an alkaline environment under elevated temperature conditions. The coefficients representing long-term rupture resistance of BFRP composites under creep stress rebars were found to be about 18% for a 50-year lifespan and 28% for 5 years. An estimated creep coefficient of 13% corresponded to the one-million-hour period. They suggested that implementing creep rupture stress limits that account for time dependency in designs of structures with limited service life could enhance the utilization of FRP bar strength.

Wang & Belarbi [19] assessed the bending functionality of concrete beams with FRP rebar reinforcement. The research commenced with the objective of creating a hybrid non-metallic reinforcement approach applied in RC beams through the integration of continuous FRP rebars and fiber-reinforced-concrete (FRC) comprising polypropylene fibers dispersed in a random manner. The experimental program involved testing twelve beams, all measuring 178 mm in width, 229 mm in height, and 2032 mm in length. Variations in FRP rebar size were included as part of the experimental design (#4 vs #8), rebar type (GFRP vs CFRP), and plain concrete vs FRC. Observed data confirmed crack openings in beams reinforced with FRP and FRC demonstrated diminished crack widths relative to FRP/plain concrete beams under the targeted service load. The magnitude of compressive strains at the uppermost fiber of the concrete in FRP/FRC beams surpassed the value of 0.004 owing to the presence of added polypropylene fibers. Additionally, an analysis of the ductility indices of FRP-reinforced members was presented. It was noted that the ductility indices of all evaluated beams exceeded the minimum requirement set at 4. Fiber addition led to an enhancement in flexural response, with ductility levels rising by more than 30% in comparison to the companion beam.

Abdalla [20] reviewed the progression regarding methods for predicting the deflection of FRP-reinforced concrete elements under flexural loading. These approaches were validated through comparison with experimental findings derived from the experimental evaluation of seven prototype concrete beams having a cross-section of 500 mm by 250 mm, featuring a clear span length of 2300 mm, that featured simple supports and were subjected to two-point loads under static conditions. Furthermore, eight experimental one-way concrete slab specimens utilizing reinforcement comprised

of FRP and conventional steel materials, measuring 3500 mm long and 1000 mm wide, were experimentally evaluated. Correspondingly, possessing an unsupported clear span of 3000 mm, two slab thickness variants were analyzed experimentally: 150 mm and 200 mm. Consideration was given to the slab depth as a key parameter, along with the reinforcement cross-sectional area and classification. The recommended analytical methods were further corroborated by experimental findings from eight concrete slabs reinforced with conventional steel, GFRP, and CFRP bars documented in prior studies. A strong correlation was observed between the theoretical predictions and experimental findings.

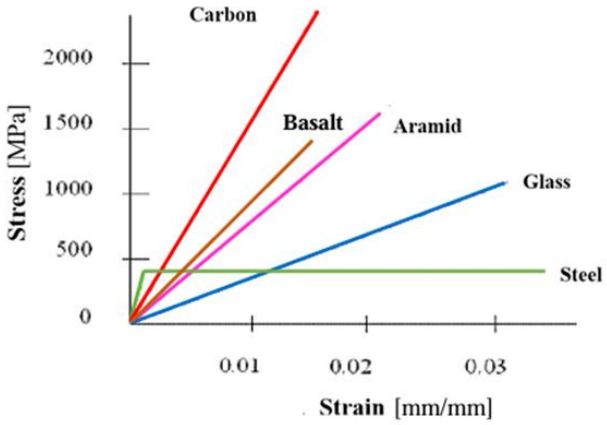

Figure 2: Stress-Strain relationship of FRP bars [10]

Table 1: Tensile properties of FRP bars [ACI.440.1R,2015][8]

Material properties	Steel	CFRP
Tensile Strength (MPa)	483-690	600-3690
Elastic Modulus (Gpa)	200	120-580
Rupture strain (%)	6-12	0.5-1.7

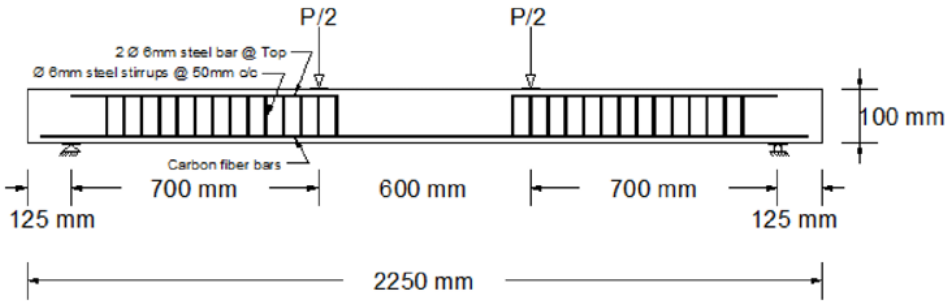

Figure 3: Test setup and detail [11]

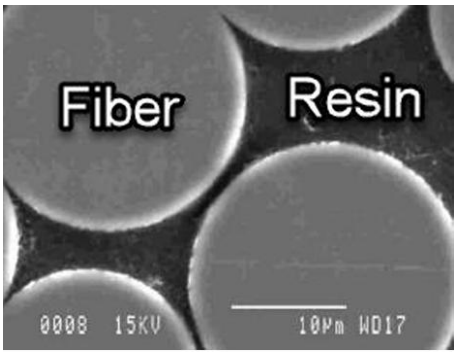

Figure 4: Microscopic structure of FRP [15]

3. Experimental Work and Methodology

3.1 Materials Properties

The material performance attributes of the reinforcing steel, FRP bars, and concrete used in the fabrication of the test specimens are compiled in Table 2 for steel and CFRP bars. The RC casting techniques were used to create the beams with a single batch of ready-mix concrete supplied by 4Bridges Company, ensuring adherence to the required specifications and quality standards. The capacity of concrete to withstand compressive stress was evaluated following the guidelines of ASTM C39/C39M-14 [21], which outlines the approved standardized testing approach for determining the ability of concrete specimens molded into cylindrical form to withstand compressive forces. After 28 days of curing, the concrete cylinders exhibited a representative compressive strength of 31.46 MPa.

Reinforcement bars arranged longitudinally at the beam's top section of the shear spans consisted of conventional deformed steel reinforcement bars having a diameter of 10 mm. Furthermore, BFRP stirrups, each measuring 8 mm in diameter, were positioned at 125 mm center-to-center intervals to mitigate shear failure in beams reinforced with CFRP.

Table 2: Properties of steel rebars and CFRP

Materials	Dimensions(mm)	Fy(Mpa)	Tensile stress Fu,ffu (Mpa)	Elastic Modulus E, Ef (GPA)	Ultimate strain	Elongation %
Steel	D10,D12,D25,D32	435	600	200	0.1-0.25	16.7
Carbon fiber reinforced polymer	D6,D8,D10,D12	-	2000	150	0.01-0.02	1.2

3.2 Sample Preparation

The research program comprises the casting and testing of 8 beams. The beam specimens were formulated in compliance with ACI 440.1R-15 and ACI 318-19. The 8 beams consist of 4 beams designed using BFRP, 4 beams designed using steel reinforcement, and 4 beams with a different rebar ratio for each beam. Group 1 contains four basalt-reinforced concrete (BSC) beams. Group 2 contains four normal steel reinforced concrete (BSN) beams.

The groups shared identical Overall height and width of 350 mm and 150 mm, respectively. Moreover, varying steel reinforcement ratios (ρf) were considered in relation to the balanced rebar ratio (ρfb) that were obtained in CFRP-reinforced concrete groups as (ρf< ρf1.4 ρfb), considering the limitations of ACI 440.1R-15 (2015) in addressing the three failure modes, tension, tension-compression, and

compression are discussed. For normal steel diverse rebar proportion conditions (ρ) with respect to this formula were obtained (As* fy = Asf * ffu), to compare them with basalt fiber reinforced polymer-reinforced concrete beams.

All beams were fabricated with a consistent concrete cover of 20 mm. Each beam measured 2500 mm in length. Standard deformed steel bars with a 10 mm diameter were employed as longitudinal reinforcement in the shear span regions at the top of the beams. Additionally, 10 mm diameter vertical stirrups were installed at 100 mm spacing configuration intended to inhibit shear failure in the conventional RC beams.

Steel bars with a deformed surface and a diameter of 10 mm were utilized as longitudinal reinforcement along the top portion of the shear spans, while carbon stirrups with a diameter of 8 mm were positioned at a center-to-center spacing of 125 mm to prevent shear failure in the beams strengthened with CFRP and were simply supported, having an effective span of 2000 mm. Table 3 shows the beam specimen groups, and Figure 5 shows the beam specimen details.

Table 3: Beam specimen groups

Group		Beam ID	Bar type	Compressive strength, f'c (MPa)	Rebar ratio
G1	G1-1	BSC-01	CFRP	30	0.3 ρfb
	G1-2	BSC-02	CFRP	30	1.1 ρfb
	G1-3	BSC-03	CFRP	30	2.43 ρfb
	G1-4	BSC-04	CFRP	30	3.65 ρfb
G2	G2-1	BSN-01	Normal steel	30	0.08 ρmax
	G2-2	BSN-02	Normal steel	30	0.12 ρmax
	G2-3	BSN-03	Normal steel	30	0.51 ρmax
	G2-4	BSN-04	Normal steel	30	0.84 ρmax

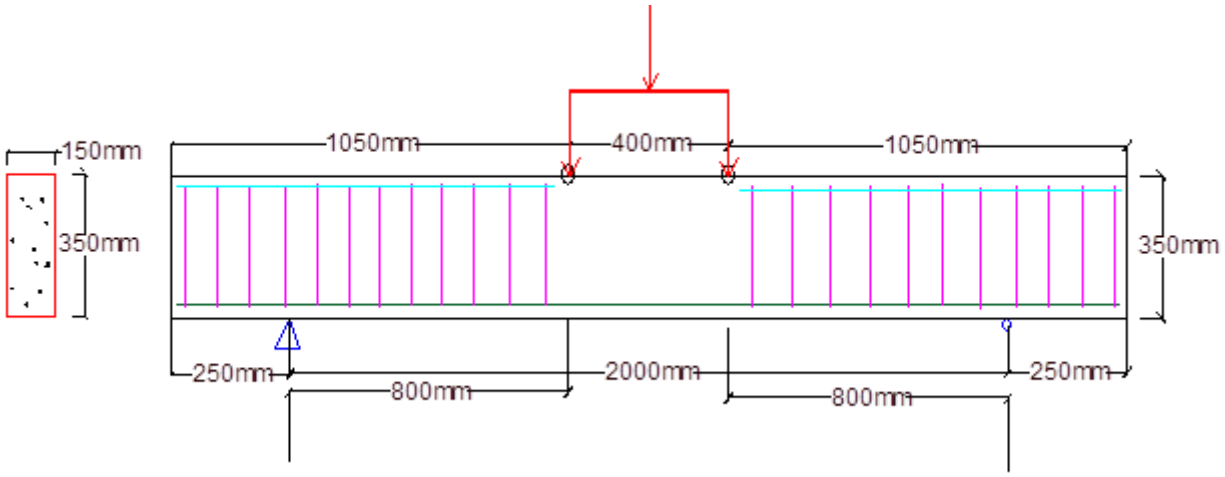

(a) Test beams' dimensions, loading position, and rebars

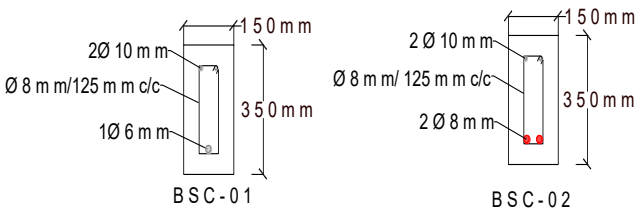

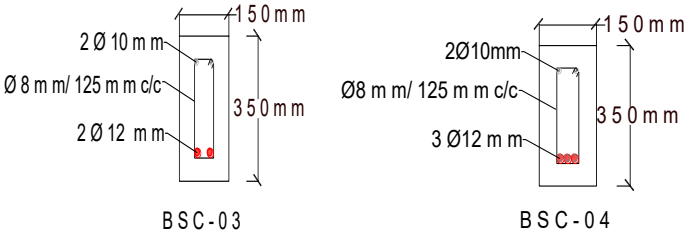

(b) Group 1(BSC) beams

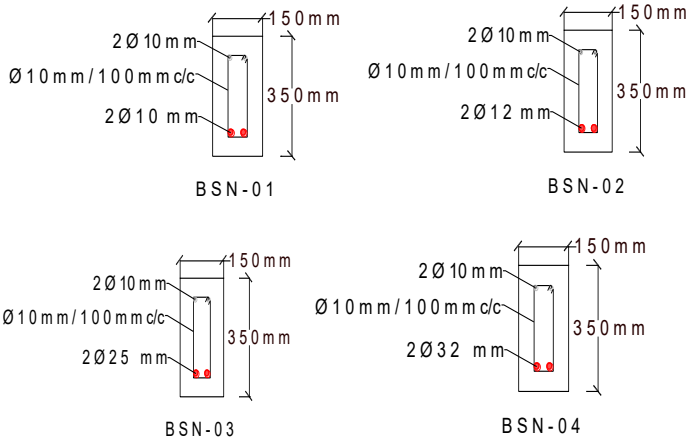

(c) Group 2(BSN) beams

Figure 5: Beam specimen details.

3.3 Test Procedure

A hydraulic jack testing machine with a capacity of 2500 kN and a loading rate of 2 kN/min was used to test twelve simply supported RC beams to failure. A static flexural test with a four-point loading arrangement was utilized in the study, as shown in Figure 6. Two concentrated loads, spaced 400 mm apart, were enforced with a symmetrical arrangement at the mid-span of each beam. Mid-span deflections were recorded using an LVDT dial gauge. Additionally, strain measurements were recorded using strain measuring devices mounted on the top surface of the beams and on the reinforcing steel bars, with data collected through a data logger.

Figure 6: Test setup

4. Equations Provided by ACI 44.1R-15

As outlined in ACI 440.1R-15, the flexural capacity of a concrete beam reinforced with FRP bars is derivable through the principles of the simultaneous satisfaction of strain compatibility and internal force equilibrium by identifying the governing failure mode, either tension or compression failure, as illustrated in Figure 7. The expected mode of failure can be predicted by comparing the actual reinforcement ratio, ρf (given in Equation 1), with the balanced reinforcement ratio, ρfb (given in Equation 2). This comparison indicates whether failure is likely to occur due to FRP rupture or concrete crushing.

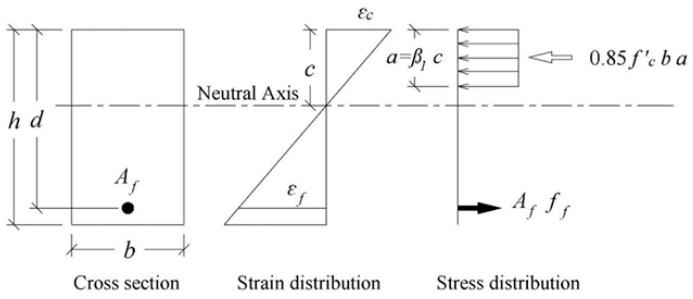

Figure 7: Stress and strain distribution [8]

(1) $$\rho f = \frac{Af}{b\ d}$$

In this expression, A_f refers to the cross-sectional area of the FRP bar, b represents the width of the rectangular cross-section, while d denotes. The location relative to the maximum compression edge of the fiber to the centroid of the FRP reinforcement.

(2) $$\rho_{fb} = 0.85\ \beta 1 \frac{f'c}{ffu} \frac{Ef * \varepsilon cu}{Ef * \varepsilon cu + ffu}$$

Here, fc′ represents the specified compressive strength of concrete, f_{fu} denotes the guaranteed tensile strength of the FRP bars, E_f is the elastic modulus of the FRP material, and ε_{cu} is the ultimate strain of concrete, typically taken as 0.3%. The coefficient β1 can be determined using the following equation:

(3) $$\beta 1 = 0.85 - 0.05 \frac{f'c - 28}{7} \geq 0.65$$

Firstly, if $\rho_f > 1.4\ \rho_{fb}$, then in the case of an over-reinforced beam, the governing failure mode is the crushing of concrete, and the flexural capacity (Mu) can be determined as outlined below:

(4) $$Mu_{,ACI} = \rho f * ff * b\ d^2\ (1 - 0.59 \frac{\rho f * ff}{f'c})$$

Where f_f is the tensile strength of the FRP bars, calculable as shown below:

(5) $$f_f = \sqrt{\frac{(Ef * \varepsilon cu)^2}{4} + \frac{0.85 * \beta 1 * f'c * Ef * \varepsilon cu}{\rho f}} - 0.5\ Ef * \varepsilon cu \leq f_{fu}$$

Secondly, if ρfb < ρf < 1.4 ρfb, the beam is in a transition zone, where concrete crushing subsequently leads to the rupture of the FRP bar, resulting in tension-compression failure. Finally, if ρf < ρfb, the beam is regarded as under-reinforced with the controlling failure mode being the rupture of the FRP bar. In this case, Mu can be estimated as follows:

(6) $$Mu_{,ACI} = Af\ *\ f_{fu}\ (d - \frac{\beta 1c}{2})$$

(7) $$\beta 1c = \frac{Af * f_f}{0.85\ f'c\ b}$$

Where c represents the distance from the extreme compression fiber to the neutral axis.

5. Results and Discussion

Figure 8 presents the load–deflection curves obtained from the empirical investigation for all control beams in Group G1 and Group G2, each featuring different longitudinal reinforcement ratios.

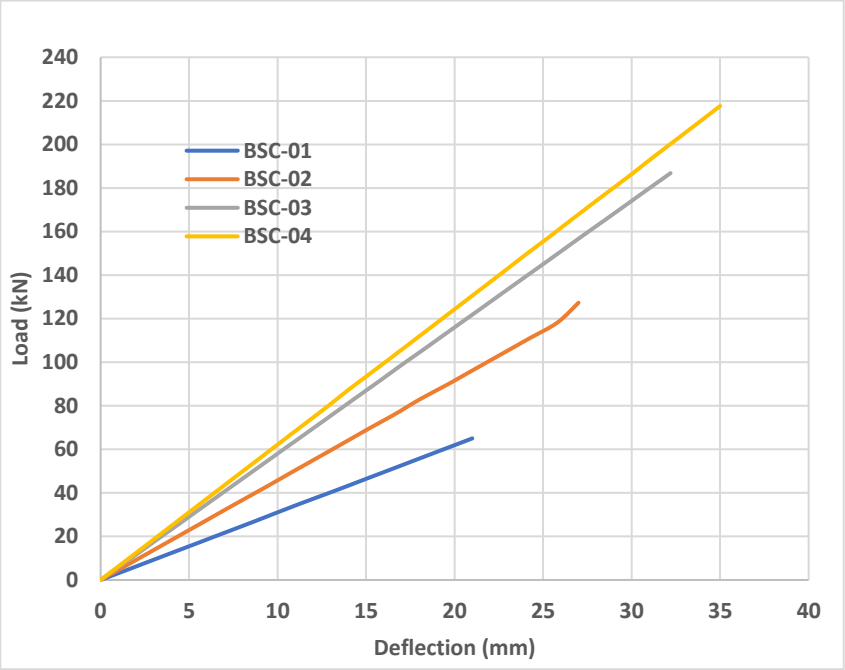

(a)

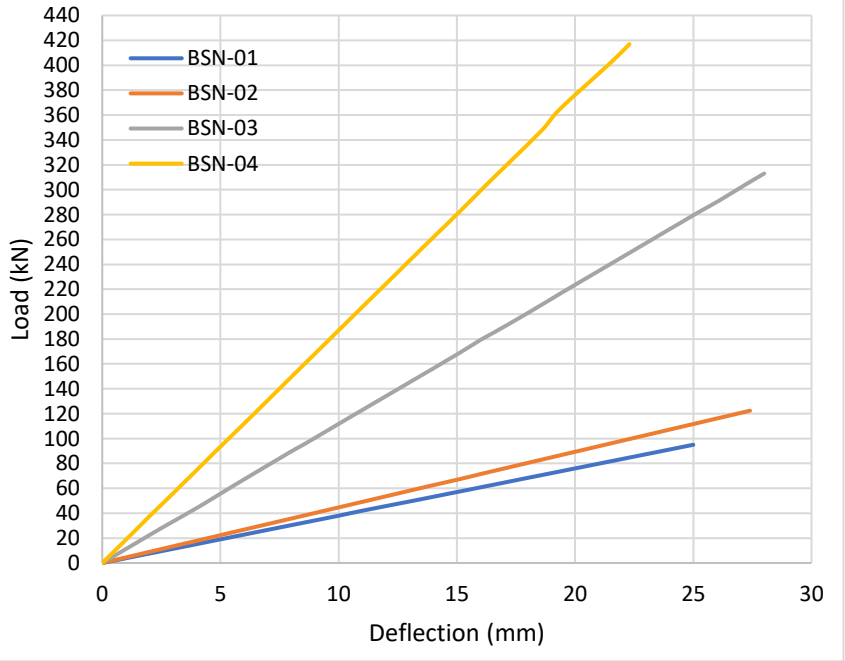

(b)

Figure 8: Load-deflection curves comparison of beams with varying longitudinal reinforcement ratios: (a) Group G1(BSC) beams, and (b) Group G2(BSN) beams

The load–deflection response curves of the tested beams are illustrated in Figure 9. The load-carrying capacity of the RC beams increased with a higher ratio of longitudinal reinforcement. Additionally, for a given load level, beams with greater longitudinal reinforcement exhibited reduced deflection.

For BSN beams, the ultimate capacity is higher than in BSC beams, and BSC beams show higher deflections than BSN beams because FRP bars have a low modulus of elasticity. That's why the deflection in BSC beams is higher than in BSN beams, as shown in Figure 10.

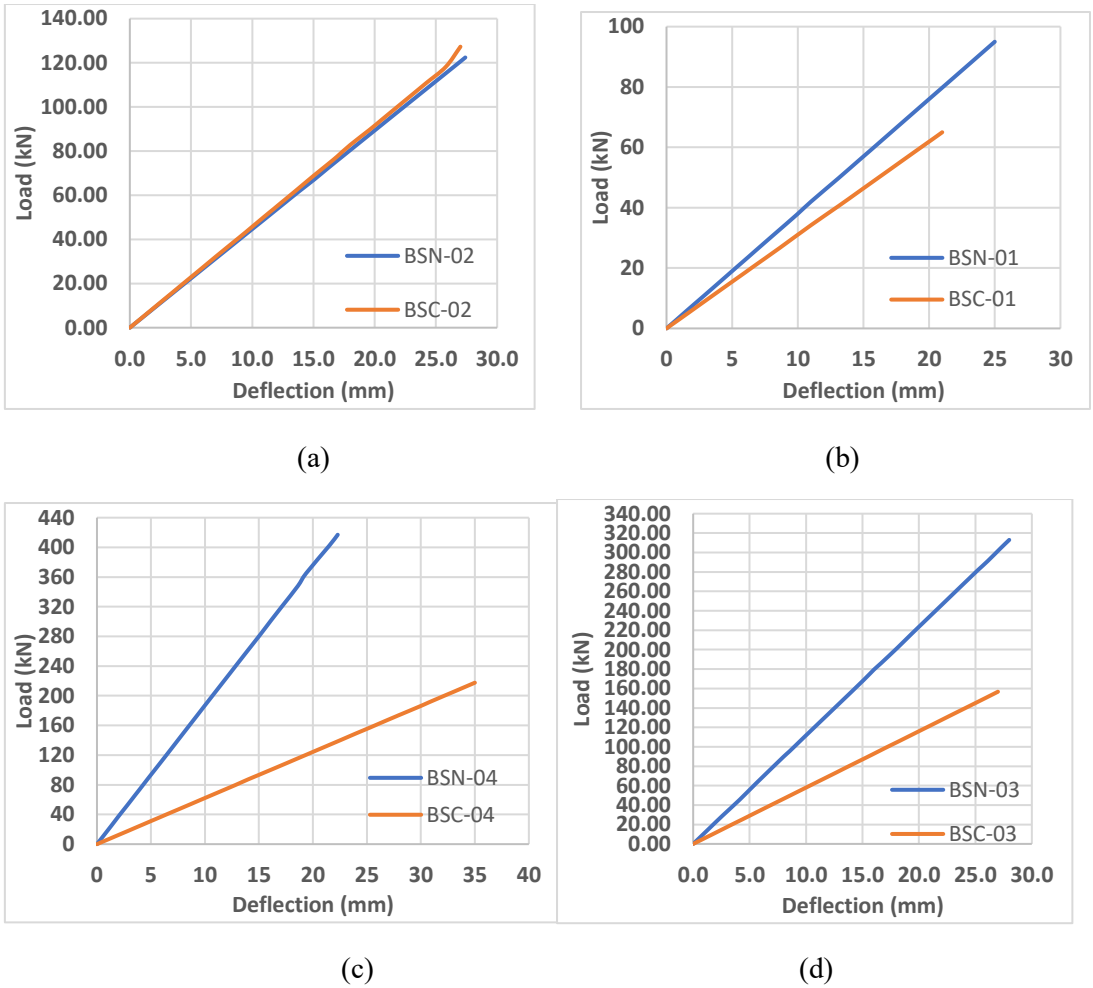

Figure 9: Load-deflection curves comparison of beams with varying longitudinal reinforcement: (a) (BSC-01) Vs. (BSN-01), and (b) (BSC-02) Vs. (BSN-02) (c) (BSC-03) Vs. (BSN-03) (d) (BSC-04) Vs. (BSN-04)

5.1 Crack Patterns

According to the failure modes described in ACI 440.1R-15 and ACI 318-19 [22] codes, the initial cracking in the OPCC beams occurred within the area of constant bending moment, directly beneath the applied point load. Following the onset of the first crack, additional cracks developed, and the width of existing cracks progressively increased as the applied load on the OPCC beams was incrementally raised.

The tested beams exhibited different behaviors since they had various amounts of tension reinforcement and different types of FRP bars.

The mid-span deflections are recorded at the maximum load condition. Furthermore, the failure modes have been determined by visual inspection. The test results are listed in Table 4.

Table 4: Results of the tested beams

Group	Beam ID	Compressive strength fc.' (MPa)	Rebar ratio condition ρ_{fb}, ρ_{max}	First crack load P_{cr} (kN)	Ultimate load P_u (kN)	Deflection Δ (mm)	Failure mode
G1	BSC-01	31.46	0.3 ρ_{fb}	44	65	21	Tension
	BSC-02	31.46	1.1 ρ_{fb}	49	127.3	27.8	Tension
	BSC-03	31.46	2.43 ρ_{fb}	52	186.8	32.2	Tension-Compression
	BSC-04	31.46	3.65 ρ_{fb}	58	217.8	35	Compression
G2	BSN-01	31.46	0.08 ρ_{max}	55.4	95	25	Tension
	BSN-02	31.46	0.12 ρ_{max}	70	122.4	27.4	Tension
	BSN-03	31.46	0.51 ρ_{max}	100	313	28	Tension
	BSN-04	31.46	0.84 ρ_{max}	131	417	22.3	Compression

For beams BSC-01, BSC-02, BSN-01, BSN-02, and BSN-03, the failure was observed in the beams primarily due to bar rupture, indicating a tensile failure mode. In contrast, Beam BSC-03 failed as a result of concrete crushing under the applied load, which progressed rapidly and was subsequently followed by the rupture of the FRP reinforcement, characterizing a combined tension-compression failure. Crack initiation coincided with the moment at which the applied load reached the beam's cracking moment. The initial cracks were vertical and aligned orthogonal to the orientation of the principal tensile stresses generated by pure bending. With further load application, the flexural cracks propagated into the shear span.

For beams BSC-04 and BSN-04, the failure was attributed to concrete crushing at the top surface under the applied load, indicating a compression failure. Compared to other failure modes, these beams exhibited a greater number of fine, closely spaced cracks. All observed failure modes are illustrated in Figure 10.

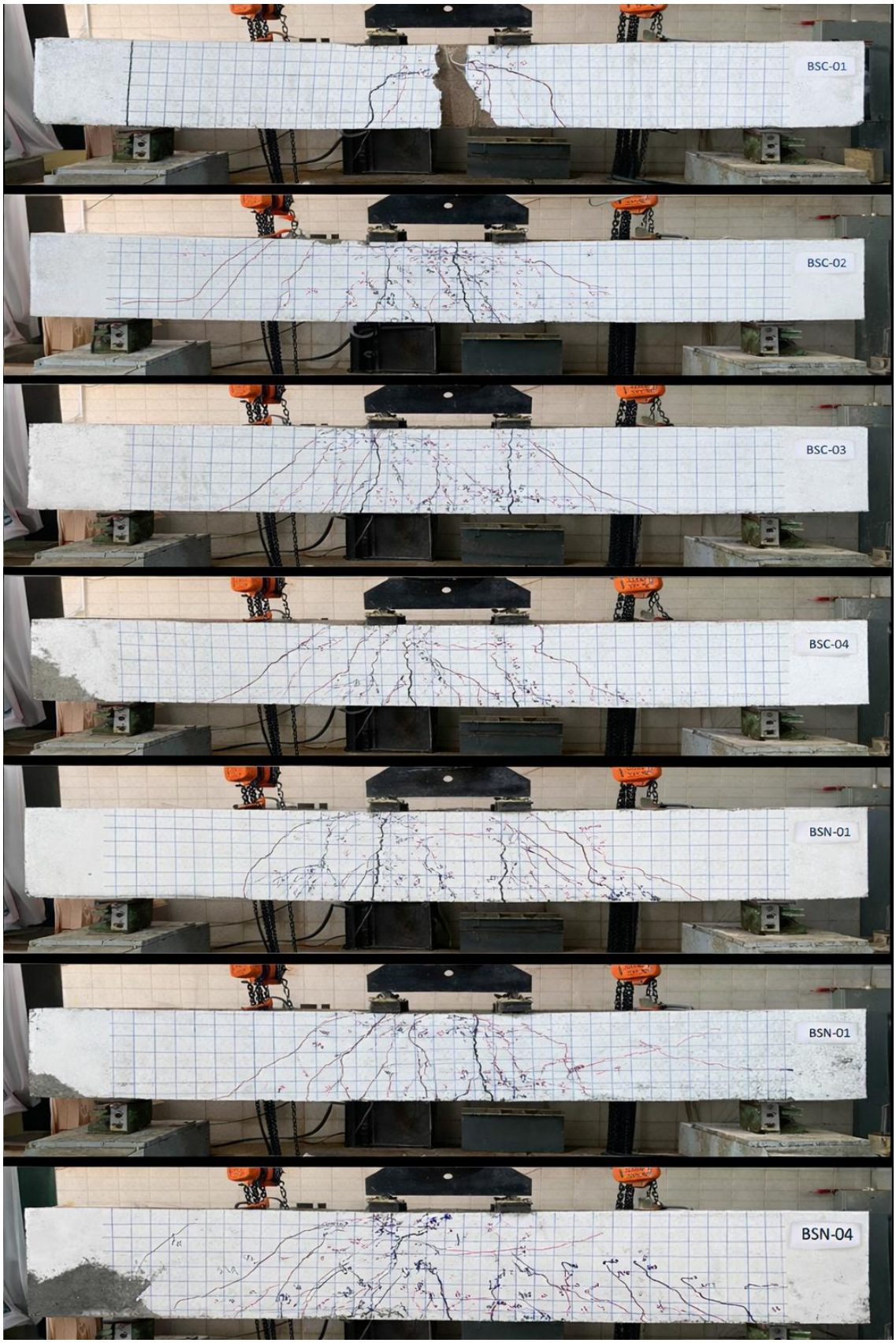

Figure 10: Crack pattern and failure mode – Group G1 and Group G2

6. Conclusions

This study used CFRP and steel bars to study the flexural behavior of RC beams.

The subsequent conclusions were derived:

The results emphasize that CFRP reinforcement is more suitable for applications where durability and corrosion resistance are critical, while steel reinforcement remains preferable in situations where higher stiffness and ductility are required. Compared to the control beams with an equivalent longitudinal reinforcement ratio, beams reinforced with steel bars exhibited a higher ultimate load capacity than those reinforced with CFRP bars as the bar ratio for steel increased from 0.08 ρmax to 0.12, 0.51, and 0.84. For CFRP, increased from 0.3 ρfb to 1.1, 2.43, and 3.65. If we compare the ultimate load, the BSN-01 ultimate load is 95 KN, while for BSC-01 it is 65KN, which means the ultimate load of BSN beams is higher than BSC beams by 31.5% on average. Increasing the rebar ratio with respect to their load deflection behavior, BSN beams were more affected by increasing the rebar ratio than BSC beams. From the curves with the increasing rebar ratio, the load for BSN beams will rise more than for BSC beams. The rebar ratio for BSN-02 is 0.12 ρmax, increased to 0.51 ρmax for BSN-03, and the ultimate load rose from 122.4 KN to 313 KN, but for BSC, with increasing rebar ratio from 1.1 ρfb to 2.43 ρfb, the ultimate load rose from 127.3 KN to 186.8 KN, which means BSN beams are more affected by increasing rebar ratio. A greater number of cracks developed under maximum loading conditions in the BSC beams than in the BSN beams. This phenomenon is influenced by the bar types. In addition, the crack widths in the BSN were more widespread than those in the BSC beams. Higher deflection occurred in beams utilizing FRP reinforcement as opposed to conventional steel reinforcement because the modulus of elasticity in FRP bars is lower than that of steel rebars. Steel reinforcement is ductile: it yields and hardens, allowing beams to redistribute stresses and carry more load before failure. CFRP is brittle: once it reaches its ultimate strain, it fails suddenly without yielding. Steel has a very strong bond with concrete due to its ribbed surface and mechanical interlock for better stress transfer.

Conflict of Interest

No conflicts of interest are reported by the authors in connection with this publication.

Acknowledgement

This study was conducted to partially satisfy the requirements for the MSc degree in Civil Engineering (Structural Engineering) at Salahaddin University-Erbil. The author extends sincere gratitude to the Civil Engineering Department and the staff of the Concrete Laboratory for their essential support and contributions.

Authors contributions

The authors confirm that all listed authors have reviewed and given their approval of the final version of the manuscript. They affirm that each contributed equally to the work and that they mutually agreed upon the sequence of authorship as presented in the manuscript.

Use of AI Tool Declaration

The authors declare that any AI tools used in the preparation of this manuscript were limited to language and readability improvement only, and were not used to generate scientific content, data, analyses, or conclusions, with full responsibility retained by the authors.

References

[1] Kadhim, A. J. & Zinkaah, H.O. Flexural behavior of hybrid (FRP/steel) reinforced concrete beams. Muthanna journal of engineering and technology. 2024, 12(1). https://doi.org/10.52113/3/eng/mjet/2024-12-01/31-42

[2] Ge WJ, Song WR, Ashour AF, Li WG, & Cao DF. Flexural performance of FRP/ steel hybrid reinforced engineered cementitious composite beams. Journal of Building Engineering. 2020, 31, 101329. https://doi.org/10.1016/j.jobe.2020.101329

[3] Gangarao, H. V. S., Taly, N., & Vijay, P. V. Reinforced concrete design with FRP composites. CRC Press. 2007. http://dx.doi.org/10.1201/9781420020199

[4] Huanzi Wang & Abdeldjelil Belarbi. Ductility characteristics of fiber-reinforced-concrete beams reinforced with FRP rebars. Construction and Building Materials. 2011, 25(5), 2391-2401. https://doi.org/10.1016/j.conbuildmat.2010.11.040

[5] Okelo, R. & Yuan, R. L. Bond strength of fiber reinforced polymer rebars in normal strength concrete. Journal of Composites for Construction. 2005, 9(3), 203-213. https://doi.org/10.1061/(ASCE)1090-02689:3(203)

[6] Benmokrane, B., Chaallal, O. & Masmoudi, R. Glass fiber reinforced plastic (GFRP) rebars for concrete structures. Construction and Building Materials. 1995, 9(6), 353-364. https://doi.otg/10.1016/0950-0618(95)00048-8

[7] Masmoudi, A., Ouezdou, M. B. & Bouaziz, J. New parameter design of GFRP RC beams. Construction and Building Materials. 2012, 29, 627-632. https://doi.org/10.1016/j.conbuildmat.2011.11.004

[8] ACI.440.1R-15 Guide for the design and construction of Concrete Reinforced with Fiber Reinforced Polymers (FRP) bars. 2015. ACI Committee 440, American Concrete Institute. Farmington Hills, MI, USA.

[9] CSA.S806-24 Design and construction of Building structures with Fiber-Reinforced Polymers. 2024. Canadian Standard Association (CSA), Ontario, Canada

[10] FICO, R. Limit States Design of Concrete Structures Reinforced with FRP Bars. 2007. PhD Thesis, University of Naples Federico II, Naples, Italy. http://dx.doi.org/10.6092/UNINA/FEDOA/1896

[11] Aziz, O. Q. & Taha, B. O. Flexure Behavior of High Strength Concrete (HSC) Beams Reinforced with Carbon Fiber Reinforced Polymer (CFRP) Rebars with and without Chopped Carbon Fiber (CCF). International journal of scientific research in knowledge. 2013, 1(6), 123-139. http://dx.doi.org/10.12983/ijsrk-2013-p123-139

[12] Rafi, M. M., Nadjai, A., & Ali, F. Experimental Testing of Concrete Beams Reinforced with Carbon FRP Bars. Journal of Composite Materials. 2007, 41(22), 2657-2673. https://doi.org/10.1177/0021998307078727

[13] FIB. FRP Reinforcement in RC Structures. 2007. ISBN 978-2-88394 080-2. https://doi.org/10.35789/fib.BULL.0038

[14] Hawileh RA, Abdalla JA, Hasan SS, Ziyada MB, Abu-Obeidah A. Models for predicting elastic modulus and tensile strength of carbon, basalt and hybrid carbon-basalt FRP laminates at elevated temperatures. Construction and building materials. 2016 Jul 1;114:364-73. https://doi.org/10.1016/j.conbuildmat.2016.03.175

[15] Mushriq Fuad Kadhim Al-Shamaa. Behavior of Lightweight Concrete Beams Reinforced with Fiber Reinforced Polymer Bars. 2010. Ph.D. dissertation, University of Technology, Baghdad.

[16] Robert, M., Cousin, P., & Benmokrane, B. Durability of GFRP reinforcing bars embedded in moist concrete. Journal of Composites for Construction. 2009, 13(2), 66-73. http://dx.doi.org/10.1061/(ASCE)1090-0268(2009)13:2(66)

[17] Sim, J. & Park, C. Characteristics of basalt fiber as a strengthening material for concrete structures. Composites Part B: Engineering. 2005, 36(6-7), 504-512. https://doi.org/10.1016/j.compositesb.2005.02.002

[18] Banibayat P, Patnaik A. Creep rupture performance of basalt fiber-reinforced polymer bars. Journal of Aerospace Engineering. 2015 May 1;28(3):04014074. https://doi.org/10.1061/(ASCE)AS.1943-5525.0000391

[19] Huanzi Wang & Abdeldjelil Belarbi. Ductility Characteristics of Fiber-Reinforced-Concrete Beams Reinforced with FRP Rebars. Construction and Building Materials. 2010, 25, 2391–2401. https://doi.org/10.1016/j.conbuildmat.2010.11.040

[20] H.A. Abdalla. Evaluation of Deflection in Concrete Members Reinforced with Fiber Reinforced Polymer (FRP) Bars. Composite Structures. 2002, 56, 63-71. https://doi.org/10.1016/S0263-8223(01)00188-X

[21] ASTM-C39/C39M. Standard Test Method for Compressive Strength of Cylindrical Concrete Specimen. 2014. ASTM International, West Conshohocken, PA, USA.

[22] American Concrete Institute (ACI 318R-19). Building Code Requirements for Structural Concrete and Commentary. 2019. Framington Hills, Michigan, USA.